An online energy management system for AC/DC residential microgrids supported by non-intrusive load monitoring

Çimen, Halil; Bazmohammadi, Najmeh; Lashab, Abderezak; Terriche, Yacine; Vasquez, Juan C.; Guerrero, Josep M.

Published in:
Applied Energy

DOI (link to publication from Publisher):
10.1016/j.apenergy.2021.118136

Publication date:
2022

Document Version
Publisher's PDF, also known as Version of record

Applied Energy 307 (2022) 118136

Contents lists available at ScienceDirect

Applied Energy

journal homepage: www.elsevier.com/locate/apenergy

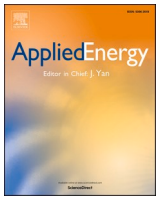

An online energy management system for AC/DC residential microgrids supported by non-intrusive load monitoring

Halil Çimen [a,*], Najmeh Bazmohammadi [a], Abderezak Lashab [a], Yacine Terriche [a], Juan C. Vasquez [a], Josep M. Guerrero [a]

[a] The Center for Research on Microgrids (CROM), AAU Energy, Aalborg University, Aalborg, Denmark

HIGHLIGHTS

- An online two-level HEMS to reduce operation cost and power consumption peaks.
- Identification of load flexibility in MG using Non-Intrusive Load Monitoring (NILM).
- Automated extraction of the occupants' power consumption patterns and preferences.
- Analyzing the performance of the proposed NILM-assisted HEMS in an AC/DC Microgrid.
- Validating the coordination of optimization and forecast systems with NILM modules.

ARTICLE INFO

Keywords:
AC/DC hybrid microgrid
Deep learning
Energy disaggregation
Energy management system
Microgrid
Non-intrusive load monitoring (NILM)
Optimization
Residential microgrid

ABSTRACT

Traditional electric energy systems are experiencing a major revolution and the main drivers of this revolution are green transition and digitalization. In this paper, an advanced system-level EMS is proposed for residential AC/DC microgrids (MGs) by taking advantage of the innovations offered by digitalization. The proposed EMS supports green transition as it is designed for an MG that includes renewable energy sources (RESs), batteries, and electric vehicles. In addition, the electricity consumption behaviors of residential users have been automatically extracted to create a more flexible MG. Deep learning-supported Non-intrusive load monitoring (NILM) algorithm is deployed to analyze and disaggregate the aggregated consumption signal of each household in the MG. A two-level EMS is designed that coordinates both households and MG components using optimization, forecasting, and NILM modules. The proposed system-level EMS has been tested in a laboratory environment in real-time. Experiments are performed considering different optimization periods and the effectiveness of the proposed EMS has been shown for different optimization horizons. Compared to a peak shaving strategy as a benchmark, the proposed EMS for 24-hour horizon provides a 12.36% reduction in the residential MG daily operation cost.

1. Introduction

During the last decade, with the increasing integration of residential wind turbines (WTs) and photovoltaic panels (PVs) as well as electric vehicles (EVs), electricity consumers have found a new role as prosumers. The possibility of locally generating and storing power along with the introduction of smart home appliances (washing machines, dishwashers, cloth dryers, electric water heaters, air conditioners, etc.) has considerably increased the flexibility on the consumer side being able to manage their power consumption pattern and participate in demand response programs. This active participation benefits both the consumers and the electricity grid in several ways. From the consumers' point of view, a lower energy cost and higher utilization of renewable energy can be expected while electricity utilities can flatten the grid load curve and reduce the stress on the system equipment, thereby increasing the system efficiency, reliability, and lifetime.

However, to exploit this flexibility, advanced home energy management systems (HEMSs) are required for monitoring and control of

* Corresponding author.
E-mail addresses: haci@energy.aau.dk (H. Çimen), naj@energy.aau.dk (N. Bazmohammadi), abl@energy.aau.dk (A. Lashab), yte@energy.aau.dk (Y. Terriche), juq@energy.aau.dk (J.C. Vasquez), joz@energy.aau.dk (J.M. Guerrero).

https://doi.org/10.1016/j.apenergy.2021.118136
Received 3 July 2021; Received in revised form 11 October 2021; Accepted 26 October 2021
Available online 13 November 2021

energy production, storage, and consumption in smart houses taking into account consumers' comfort as well as their economical and environmental concerns [1]. Accordingly, many studies have been dedicated to HEMSs and residential energy management over the last decade. The developed strategies are either for a single house [2–4] or multiple households in a residential area [5,6]. Moreover, demand-side flexibility management can be achieved through an aggregator as an intermediary entity between consumers and distribution system operators [7,8].

In [2], an energy management strategy for a residential microgrid (MG) is proposed to reduce the system costs and obtain a smoother grid power profile. Instead of appliance-level analysis, the aggregated energy consumption profile is forecasted and optimization is performed. In [3], given the uncertainty of customers' behavior, a load scheduling method is proposed taking into account energy cost and a satisfaction function through the robust intervals of different appliances. Customers are required to preset the start and end times of the interval that the appliance can be scheduled in. In [4], a two-stage HEMS is proposed that aims at minimizing the deviation of electricity demand from a reference trajectory received from the aggregator. To reduce the computational complexity, hourly and intra-hourly appliance scheduling are performed at the first and second stages, respectively. In [5], a HEMS is proposed for multiple houses with EVs, PVs, air conditioners, and water heaters. The problem is formulated as a multi-objective optimization problem to maximize consumer satisfaction (in terms of room and water temperature) and minimize energy cost and the load peak-to-average ratio. A Pareto tribe evolutionary algorithm is used to find the solution set.

In general, HEMSs deal with a load management problem that is formulated in the form of a multi-criteria optimization problem subject to several technical and operational constraints derived from the available flexibility resources and user preferences. In this regard, different controllable appliances should be identified and their power consumption, operating interval, and possibility for operation interruption should be provided to the HEMS. Given the varying power consumption patterns of residential consumers in different hours of the day, days of the week, and times of the year, adjusting these settings manually is a tedious task. In [6], given the difficulty of a priori setting of customer comfort without distinguishing among different customers with various needs, a HEMS with profile characterization of smart appliances is proposed. The goal is to minimize the household energy costs and users' annoyance levels using a quality of experience-driven approach. Consumers are asked to register their tendency to shift the loads or changing the temperature settings over a training period. However, automating this process will minimize user intervention by adaptively learning occupants' power consumption patterns and preferences. Equipping HEMSs with this capability requires advanced learning techniques and power consumption data acquisition of different household appliances. In this regard, Non-Intrusive Load Monitoring (NILM), also referred to as energy disaggregation, provides a promising solution.

1.1. Literature review for NILM

NILM, first proposed by Hart [9], is a technique to identify the power consumption of different appliances and their activation intervals by disaggregating the power consumption profile of the house, thereby avoiding the installation and maintenance cost of separate sensors for single appliances that are needed in intrusive techniques [10]. Having appliance-level data allows customers to have detailed information about their consumption and thus make more informed decisions. On the other hand, electricity utilities might benefit from the knowledge of appliance-level consumption preferences to estimate the potential capacity for demand response programs and adjusting their pricing strategies as well as policymaking [11].

NILM analysis can be performed with both high and low sampling frequency measurements [12]. But there are already thousands of smart meters installed. To exploit this potential, recent NILM studies are focusing on low sampling frequency measurements. NILM analysis is performed in two different ways: non-event-based (state-based) and event-based. Non-event-based approaches represent the appliances as finite state machines. The operation of the devices is modeled by designing state transition models. One of the most widely used non-event-based approaches is the Hidden Markov Model (HMM) and its variants such as Factorial HMM, Conditional Factorial HMM, Additive Factorial HMM, Hierarchical HMM, and Super-state HMM [13–17]. The most important disadvantage of HMM-based methods is that, as the number of appliances increases, the complexity of the model increases exponentially [18]. On the other hand, event-based approaches rely on event detection and feature extraction. The authors of [19] have developed an event-based appliance recognition algorithm working in the frequency domain and deployed a filtering process to detect state transitions. To extract high-level features, a multiscale wavelet packet tree has been used. In [20], the detection of simultaneous switching devices, which is one of the important research topics of NILM analysis, has been evaluated. An adaptive-window-based detection approach is applied to detect the events, and a deep dictionary learning model is used in the real-time load monitoring architecture. In order to increase the quality of extracted features, appliance power signals have been transformed into 2D space and short histograms representing individual appliance consumption have been extracted in [21]. However the aforementioned event-based methods need event detection and feature extraction process which might be time-consuming. Besides, they are designed only for load identification. However, to design an effective EMS, it is necessary not only to identify the loads but also to extract their power consumption.

With the increasing availability of public datasets, machine learning methods started to be applied frequently in the field. Convolutional neural networks (CNNs), recurrent neural networks (RNNs), and Generative Adversarial Networks are the most widely used deep learning methods in the literature [22–25]. RNNs are used to analyze time series because they can analyze temporal dependencies. This feature is significant for NILM because the energy consumption of the devices is a time series and is related to the past consumption profile [26]. CNNs, on the other hand, can extract features hierarchically from raw data [27]. Therefore, it enables the analysis of smart meter signals without exhausting preprocessing. In order to increase the generalization of deep learning models, the authors of [28] have used data augmentation to generate synthetic data for training a CNN-based NILM model. The proposed data augmentation technique works by combining on and off-durations of a target appliance from various datasets. Considering that having a large amount of labeled data might not be always practical, the authors of [29] have used a spiking neural network that only requires the user to label one instance for each appliance while adapting to a new household.

1.2. Literature review for NILM assisted HEMS

Given the ability of NILM to identify appliance usage patterns in a non-intrusive manner, deploying it in a HEMS will help improve its efficiency and autonomy [30]. However, this is a rather new concept that has been investigated in few studies. In [31], a NILM-based HEMS is proposed in which NILM is used to identify the preferred usage time of different appliances and their wattage. Day-ahead load scheduling is formulated in the multi-objective optimization framework with conflicting objectives of cost and residents' comfort. It is shown that total electricity payments and load peak-to-average ratio are reduced with deploying this method. Moreover, authors in [32] propose a deep neural network-based NILM integrated with EMS. Power consumption and operating status of different appliances are identified using a multi-task neural network. Afterward, average power consumption, operation cycle, daily usage frequency, and desired usage periods for different appliances are estimated. The proposed method is evaluated for the EMS of a household MG with WT, PV, and energy storage system (ESS).

According to the results, operation cost and customer satisfaction have been considerably improved. Incorporating NILM for demand response flexibility estimation is analyzed in [33]. An unsupervised NILM algorithm based on a combinatorial optimization problem is proposed to disaggregate the power consumption of residential consumers. The demand response flexibility of a region is quantified by comparing the load patterns before and after implementing demand response programs. According to their study, EVs provide the most flexibility for the demand response programs. Another residential energy flexibility study supported by NILM is proposed in [34]. An unsupervised algorithm is deployed to disaggregate the controllable load patterns. Then flexibility characterization is determined considering the consumers' usage behavior. The proposed method is verified in an individual building level and aggregated level including 50 residential buildings. The authors of [35] propose a NILM-assisted demand response program. Operation information of controllable loads, which are air conditioning units and EVs, is extracted by NILM. The obtained results are sent to the utility as feedback showing whether the enrolled appliances comply with the demand response signals or not.

As seen in the above-mentioned studies, NILM is basically a signal processing problem, where most of the studies have focused on increasing its analysis accuracy. However, how to benefit from NILM, where and how to use the results have not been adequately addressed.

In this paper, an advanced system-level NILM-assisted EMS is designed for hybrid AC/DC residential MGs. The goal is to automate the load profile characterization by learning occupants' power consumption patterns and preferences and maximize the consumers' benefits using the maximum available flexibility sources. The main contributions of the paper are as follows:

- Designing an online two-level HEMS for reducing the consumers' electricity bill and the power consumption peaks while considering occupants' preferences by exploiting different flexibility sources in residential MGs.
- Identification of different flexibility sources in a residential MG including the flexible loads and their power consumption and preferred usage intervals with the help of a non-intrusive tool to minimize sensor cost and user intervention.
- Integrating a deep learning-based NILM algorithm with the HEMS to automate extracting the occupants' power consumption patterns and preferences.
- Analyzing the performance of the proposed NILM-assisted HEMS in a hybrid AC/DC MG taking into account the increasing use of flexible units such as home appliances, WTs, PVs, and EVs.
- Validating the coordination of optimization and forecast systems with NILM modules in a real-time EMS at the system level with HIL tests in a laboratory environment.

2. The architecture of the residential AC/DC MG

MGs are known as small-scale power systems including different types of distributed generation units and storage devices that are used in many different areas such as aviation, automotive, military, and households [36]. Considering that 27.4% of the electrical energy generated worldwide is consumed by households, it is understood that households have great potential in terms of energy savings [37]. By using small capacity RESs and ESSs, each house becomes a small MG, being able to meet its energy needs on its own, and become an active participant in the energy sector. Another advantage of households is that there are a large number of controllable loads inside. Shifting the operation time of appliances according to electricity price signals provides a financial gain to the consumers. In addition, it may positively contribute to the peak load problem faced by the distribution network in the evening hours. In this regard, EMSs play an important role, especially for residential MGs. By having information such as power consumption profiles of households, available power generation of RESs, and real-time electricity prices, more effective EMSs can be designed. In this paper, considering that the households have a great potential in energy saving, a residential AC/DC MG which is shown in Fig. 1 is analyzed [38].

The analyzed MG includes more than one apartment. Therefore, the WT, PV, ESS, and EV charging station belong to the entire building. The reason why a hybrid MG is analyzed is the advantages of DC-based power systems in terms of simplicity and efficiency [39]. If PVs and ESSs are connected to the DC bus, there will be no need for an extra DC/AC conversion process, so the cost is reduced and efficiency is increased by using fewer power converters. In addition, the increase in the use of EVs and the fact that most of the charging units are DC is another advantage. However, it does not seem possible for now to use only DC in residential buildings. The reason is that DC systems to be used in buildings are not yet subject to a standardized regulation in terms of protection, control, and operation. For this reason, the MG is designed by using a DC and an AC bus so that the apartments in the building are fed without extra design. The AC and DC buses are connected by a 3-phase interlink converter. With the help of an interlink converter, power transfer between busbars is regulated.

3. Proposed energy management system

3.1. Introduction of EMS architecture

EMSs can be defined as computer-aided systems that monitor MGs and enable them to operate in an economical, reliable, and sustainable manner. The energy management algorithm of the EMS tries to determine the optimum operating points of MGs equipment considering their technical and operational constraints as well as information of electricity demand and market prices to ensure optimal system operation. Many different operation management strategies such as generation planning, energy-saving, reactive power support, and frequency regulation have been implemented before [40]. Although EMS can be designed for different purposes, in this paper, it is aimed to achieve the optimum generation-consumption balance by monitoring and coordinating all units in a residential MG in an online framework. To achieve

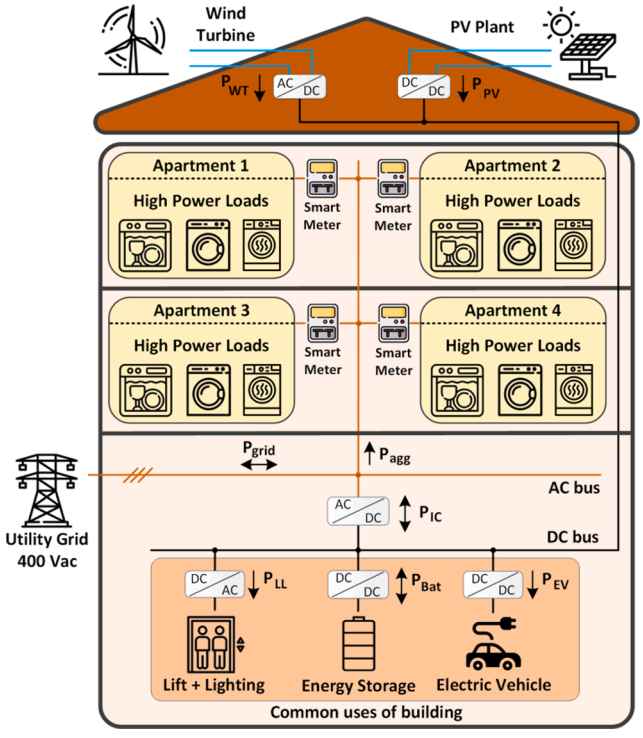

Fig. 1. The architecture of the residential AC/DC MG.

this goal, an online EMS, which is shown in Fig. 2, is proposed.

The proposed EMS consists of 5 different modules. The first of these is the *Data storage and Data Acquisition / Human-Machine Interface* (*DAQ/HMI*). Bidirectional communication is established with the MG, and data exchange is provided through this module. *HMI* allows all the data collected from the MG to be visualized. If needed, input values can be modified based on the required data. This module reads the necessary measurements from the MG, shares them with other modules, and sends back the output signals of EMS to the MG. Moreover, all the collected data are stored in this module.

The second module is the *Data Preprocessing* module that enables data received from the storage module to be converted into the required structure before being distributed to other modules. Since the *NILM*, *Forecast,* and *Optimization* modules need different data structures, using a preprocessing module will facilitate appropriate coordination and data sharing.

The third module is the *NILM* module which uses the smart meter signals of the apartments as input. The read signals are analyzed using various mathematical or pattern recognition methods and appliance-level data are extracted, which enables the analysis of the energy consumption behavior of each apartment. Thus, considering the preferences of the consumers, their electricity bills can be reduced and their comfort level can be maximized.

The *Forecast* module provides the necessary generation and consumption forecasts for the operation planning of the MG. Some variables such as renewable energy generation, household electricity demand, and the use of EV charging stations have a probabilistic nature. However, to operate the MG in an optimum way, it is necessary to know the generation and consumption information of all units in the system in advance. This module helps the *Optimization* module to make a more efficient energy management strategy by making forecasts. As the error of the forecasts decreases, the efficiency of the EMS will increase.

The last module is the *Optimization* module in which the optimization process is performed for a previously determined horizon and the operating set-points of the MG units are determined. It is aimed that the MG will be operated optimally by ensuring that the units will follow the set-points.

3.2. Interaction of modules

The operation principle and interaction of different modules are shown in Fig. 3. First of all, with the help of the *DAQ/HMI* module, the necessary measurements are collected from the MG and stored in the database. In the next step, forecasting and NILM are performed simultaneously. The *Forecast* module requests the data from the *Preprocessing* module and makes power generation-consumption estimations. NILM is performed only at the beginning of the day and it analyzes the consumer's preferences. After the forecasting and NILM processes are completed, the obtained data are concatenated and sent to the *Optimization* module through the *Data Preprocessing* module. At this stage, an optimization process is carried out by taking into account the generation-consumption forecast, electricity price, state-of-charge (*SoC*)

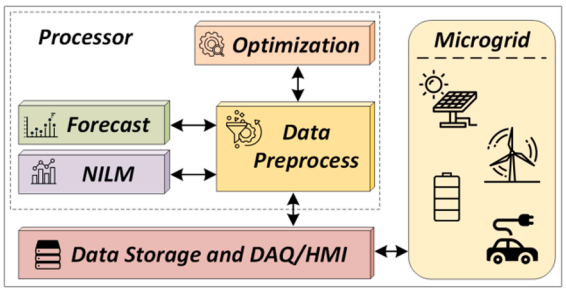

Fig. 2. The architecture of the proposed EMS.

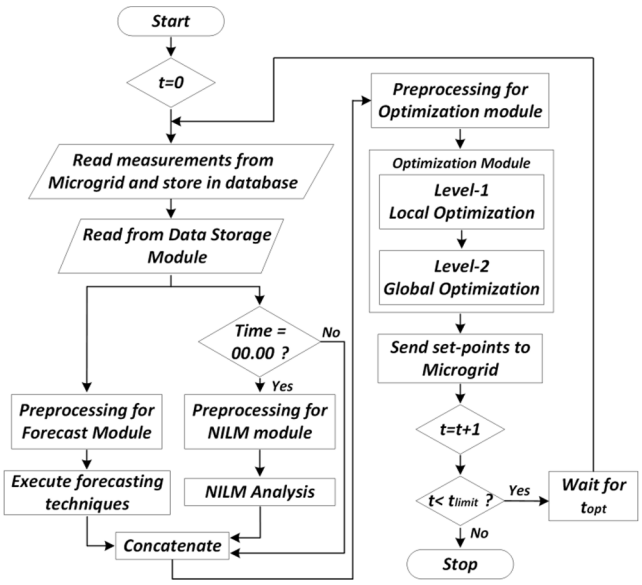

Fig. 3. Operation flowchart of the proposed EMS.

of battery, and system constraints. Optimization is performed for a period defined as the optimization horizon (H) with a time step of Δh, which is shown in Fig. 4. Once the optimization is completed, the operating set-points are sent back to the MG through *DAQ/HMI* module.

For an online EMS, all operation steps described above are repeated after waiting a user-specified time which is called the optimization step (t_{opt}). For each iteration, the necessary sensor measurements are obtained, new forecasts are made, and the optimization process is performed again. In this way, the inconsistency between forecasted and actual values is minimized as it will be easier to forecast the near future. This process continues until a user-defined time (t_{limit}).

3.3. NILM

NILM, also referred to as energy disaggregation, is the process of obtaining appliance-level data by disaggregating the total household electricity consumption measured by the main meter using various signal processing or pattern recognition methods [9]. Rather than using a separate sensor for each appliance, the aggregated signal which is the total energy consumption of a household is monitored. Since the main meter data is only needed for analysis, it is less costly than the other monitoring systems [10]. NILM can also be thought of as a filter as shown in Fig. 5.

The NILM problem is formulated as follows:

$$p_{sm}(t) = \sum_{n \in N} s_n(t) \cdot p_n(t) + e(t) \tag{1}$$

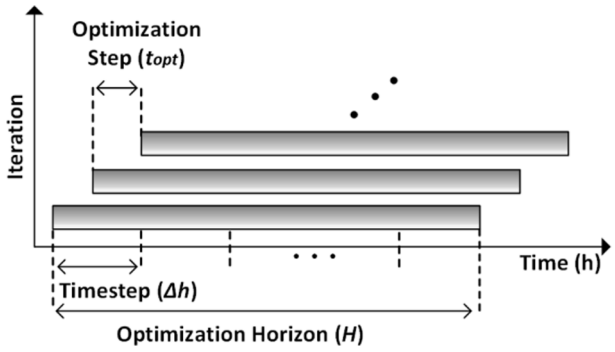

Fig. 4. Optimization windows.

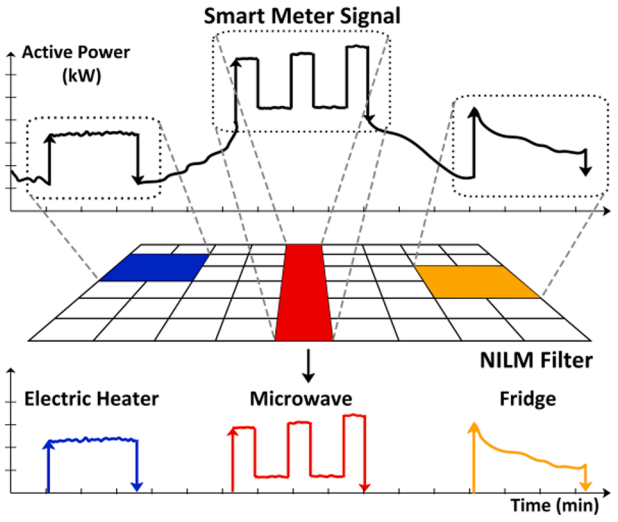

Fig. 5. NILM process.

where $p_{sm}(t)$ indicates the aggregated active power consumption read from the smart meter at time instant t, s_n is a binary variable showing whether appliance n is running, and p_n indicates the active power consumption of appliance n. $e(t)$ is the measurement error and N is the total number of appliances in the household. As a result of NILM analysis, s_n and p_n are expected to be extracted with high accuracy.

By using NILM, statistical data about appliances (usage frequency, consumed energy, usage time, etc.) can be obtained, and this information can be used for appliance scheduling, thereby energy saving. With the integration of the NILM in EMS, consumers' electricity consumption habits can be extracted. Considering these habits, customers can participate in various demand response applications that will be offered by the utility grid. One of the easiest ways to reduce the electricity bill is to shift the use of appliances to periods where the price of electricity is cheaper. However, it is not always possible for customers to manually program their consumption by following the variation of electricity prices. Studies show that consumers who want to change their energy consumption behaviors to reduce their bills are either the elderly or prudential people [41]. Other consumers are either too busy or are unsure of how to respond to grid signals. For this reason, automation has a big role in demand response applications. The lifestyles of each consumer must be taken into account to design and implement an automated management strategy for different households. By using the NILM, the life habits and consumption behaviors of each customer can be learned and consumer-specific optimization can be made. In this way, both energy costs can be reduced and consumer comfort can be maximized.

The aggregated signal is sufficient to extract appliance-level information and it can be easily obtained with the help of smart meters. The widespread use of smart meters means that the data that can be used for analysis is abundant. Therefore, data-driven techniques can be a viable solution to solve this problem. In this paper, the energy consumption behavior of the consumers in the apartment is analyzed using a Multi-task neural network model which extracts both power consumption profiles and the status of appliances. Since the main purpose of this paper is to explain the operation principle of the proposed online EMS and to implement it in real-time, the deep learning model will not be explained in detail. However, the NILM model was presented and implemented in our previous paper [32].

1) Extracting of appliance parameters

Once the NILM analysis is complete, some appliance parameters need to be extracted for use in the EMS. These are the average power consumption (*PC*), the average operation time (*OT*), the average number of daily uses (NU), and the most preferred operation interval (*POI*). These parameters are extracted by analyzing the NILM outputs using the following formulas:

$$PC_n = \frac{\sum_{u_n \in U_n}[(\sum_{t=\alpha_{u_n}}^{\beta_{u_n}} \widehat{p}_n(t))/(\beta_{u_n} - \alpha_{u_n})]}{U_n} \tag{2}$$

$$OT_n = \frac{\sum_{u_n \in U_n}(\beta_{u_n} - \alpha_{u_n})}{U_n} \tag{3}$$

$$NU_n = \frac{U_n}{AP} \tag{4}$$

where U_n is the total number of uses for appliance n detected during the analysis period. $[\alpha_{un}, \beta_{un}]$ indicates the time interval the appliance n is actively operating in the u^{th} usage. The *PC* is calculated by dividing the sum of the average power consumed by the appliance during each operating period by the total number of uses U_n. $\widehat{p}_n(t)$ indicates the NILM estimation of active power consumption of appliance n for time t. Similar to the *PC*, the *OT* is calculated by dividing the sum of each run time by the total number of uses. The *NU* is obtained by dividing the total use number of the appliance by the daily analysis period *AP*. The *NU* is an important parameter because the usage number of appliances used in an apartment with five people and an apartment with a single person can be significantly different. The *POI*, which indicates the period in which the appliances are used most frequently, is a statistical value spread over 24 h. Therefore, the *POI* will be defined with a probability density function (PDF).

3.4. Optimization procedure

In this paper, a two-level optimization problem for AC/DC residential MGs is proposed and it is mathematically modeled. In this way, it is aimed to meet the demands of both the distribution system operator and the customers at the same time.

1) Level 1 - local optimization

The first level of optimization aims to minimize the electricity bills of the apartments in the building individually by shifting the usage time of the appliances. For this reason, the objective function of Level 1 is defined as follows:

$$Min\left\{OF_{1,d} = \sum_{t=1}^{24} RTP(t) \cdot P_{load,d}(t)\right\} \tag{5}$$

where *RTP* stands for the real-time price of the utility grid, $P_{load,d}(t)$ indicates the active power consumption of apartment d at time t and it is determined by scheduling the runtime of appliances. Before starting the optimization, consumers who accept the scheduling of the appliances in the home, i.e., those who want to participate in the EMS, should be

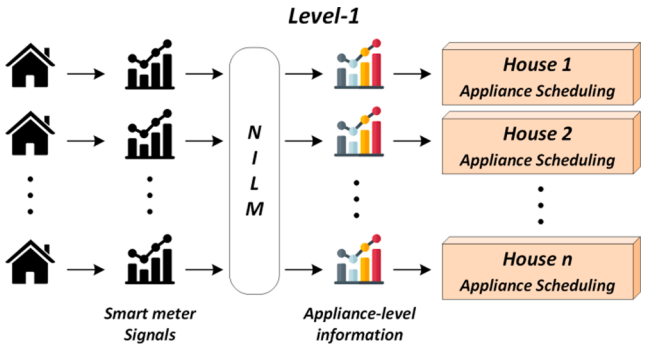

Fig. 6. Level 1 - Local optimization.

determined. Therefore, local optimization is applied only for consumers who want to participate in the EMS, as shown in Fig. 6. Local optimization is applied separately since consumer behavior can be significantly different.

First, the smart meter signals of the consumers are read through *DAQ/HMI* module and analyzed with the help of the *NILM* module. Following this analysis, the appliance-level energy consumption information of the consumers is obtained.

The appliances in the apartments are divided into two categories as non-shiftable and shiftable loads. Non-shiftable loads such as ovens and hair dryers are devices that the consumer should use whenever they need. However, the run time of shiftable loads such as washing machines and dishwashers can be shifted. Another example is thermostatically-controlled loads such as air conditioners and refrigerators which can be controlled to maintain the temperatures within certain limits [42]. Significant energy savings can be achieved by shifting the runtime of shiftable appliances according to RTP and user preferences. Shiftable tasks can be planned according to several operating requirements. The required constraints are defined as follows [43]:

$$\sum_{t=1}^{24} s_n(t) = OT_n \tag{6}$$

$$\sum_{t=1}^{24} |\, s_n(t) - s_n(t-1)\,| \leqslant 2 \tag{7}$$

$$\sum_{t=1}^{24} s_m(t)\cdot\gamma(\lambda - OT_n + \sum_{\bar{t}=1}^{t} s_n(\bar{t})) = OT_m \tag{8}$$

$$P_{load}(t) = \sum_{k \in NN} P_k(t) + \sum_{l \in NS} P_l(t)\cdot s_l(t) \leqslant P_{load}^{max} \tag{9}$$

where s is a binary variable showing that the appliance is operating or not. Equation (6) ensures that appliance n finishes its operation within the determined OT, while (7) ensures that uninterruptible appliances such as washing machines and dishwashers operate without interruption. The operation of some appliances, such as a dryer, depends on the washing machine running before it. Equation (8) ensures the operation order of such dependent appliances. γ indicates a unit step function while λ defines a positive number less than one. Besides, equation (9) guarantees that the instantaneous power consumption is below the upper limit, taking into account the capacity of the protection equipment. Here, *NN* and *NS* refer to the number of unshiftable and shiftable loads in the household, respectively.

The local optimization phase is completed by applying (5)-(9) separately for each user participating in the EMS. Thus, the scheduled consumption profiles for the participating users (P_{Pa}) during the next 24-hour scheduling interval are obtained. The consumption profiles of non-participating users (P_{NPa}) are determined by the *Forecast* module. The output of Level 1 is an aggregated consumption profile, which is the sum of the next day 24-hour consumption profiles of all apartments as follows. Therefore, Level 1 is performed only once a day to plan the next day's power consumption.

$$P_{agg}(t) = P_{Pa}(t) + P_{NPa}(t) \qquad t = 1, \ldots, 24 \tag{10}$$

2) Level 2 - global optimization

At this level, the problem is viewed from a broader perspective. Details regarding the operation of the MG, such as generation planning of the units, evaluation of *SoC* of the batteries and charge status, and power exchange with the grid, are handled at this stage. The architecture of the secondary level optimization is shown in Fig. 7.

At this stage, the result of the optimization performed at Level-1 is transmitted to the global optimization unit. In addition, the power generation and consumption estimations obtained from the *Forecast* module are also sent to the *Optimization* module and the optimization process is performed for the MG. Two different objective functions are taken into account for the operation cost of the MG (F_1) and grid power Peak-to-Average Ratio (*PAR*) which is modeled with the standard deviation (*std*) of the received power from the main grid (F_2) [5]. The first objective function is minimized to reduce the operating cost of the MG, and the second objective deals with the new peaks which may appear after power scheduling. These two functions are expressed as follows:

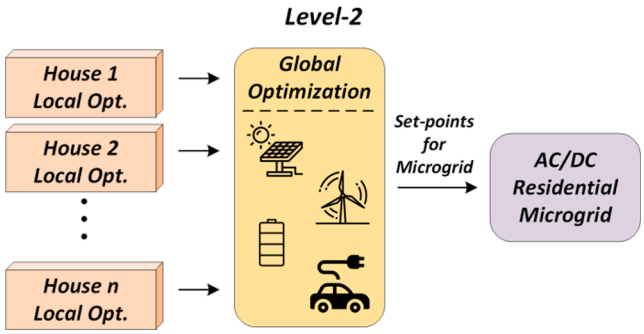

Fig. 7. Level 2 - Global optimization.

$$F_1 = \sum_{h \in H} RTP(h)\cdot P_{grid}(h) \tag{11}$$

$$F_2 = std(P_{grid}) \tag{12}$$

where H indicates the optimization horizon shown in Fig. 4, $P_{grid}(h)$ is the power exchanged with the utility grid at a given time h. By optimizing the operation cost, the consumers residing in the building can get the maximum economical benefit from the MG. The second term is defined as the *std* of the power drawn from the grid. The smaller the F_2 value, the smoother the power exchange profile. By considering these two functions, a multi-objective optimization problem is defined for the global optimization as follows:

$$Min \quad F_i(x) \quad i = 1 : N_{obj} \tag{13}$$

where F_i is the i^{th} objective function and N_{obj} shows the number of objectives which is two in this case. Unlike single-objective optimization problems, which result in a single optimal solution, multi-objective optimization problems lead to a set of optimal solutions called Pareto optimal set or non-dominated solutions. Considering two feasible solutions of $\times$ and y, it is said that $\times$ dominates y if $F_i(x) \leq F_i(y)$ for all $i = 1$: N_{obj} and $F_j(x) < F_j(y)$ for at least one objective in a minimization problem. In order to explore the Pareto optimal set, the weighted sum objective function of OF_2 is formed as follows:

$$Min\{OF_2 = w_1\cdot F_1 + w_2\cdot F_2\} \tag{14}$$

The coefficients w_1 and w_2 are weighting coefficients that are used to assign the relative importance of different objectives. After finding the Pareto optimal set, a compromise solution can be found considering the decision-maker preferences. In this paper, the value of a linear fuzzy membership function is calculated for all non-dominated solutions as follows:

$$\mu_i = \begin{cases} \dfrac{F_i^{Max} - F_i}{F_i^{Max} - F_i^{min}} & F_i^{min} \leqslant F_i \leqslant F_i^{Max} \\ 0 & otherwise \end{cases} \tag{15}$$

in which, F_i^{min} and F_i^{Max} are the minimum and the maximum values of the i^{th} objective function, respectively [44]. The final solution is selected from the point of view of a conservative decision-maker that tries to maximize the minimum satisfaction of all objective functions considering the N_s non-dominated solutions as represented below [45]:

$$\max_{k=1:N_s} \min_{i=1:N_{obj}} \mu_i^k \tag{16}$$

The multi-objective optimization problem is subjected to several constraints. The first of these constraints is the power generation-demand balance of the MG. This balance should be maintained separately for AC and DC busbars with the help of the following equations:

$$P_{WT}(h) + P_{PV}(h) - P_{bat}(h) - P_{EV}(h) - P_{LL}(h) - P_{IC}(h) = 0 \tag{17}$$

$$P_{grid}(h) + P_{IC}(h) - P_{agg}(h) = 0 \tag{18}$$

Equation (17) is defined for the energy balance of the DC bus. The aim is to ensure that the power injected and drawn from the busbars at time h is equal, according to Kirchoff's current law. The wind turbine (P_{WT}) and solar panels (P_{PV}) inject current into the DC bus, while the electric vehicle (P_{EV}) and lift/lighting (P_{LL}) draw power from the DC bus. The sign of the interlink converter (P_{IC}) is considered negative when it draws power from the DC bus. Similar to the DC bus, the energy balance of the AC bus is ensured by (18).

The next constraint is the upper and lower operating limits of the units. The power generation of wind turbine and solar power plant, the power drawn from and sold to the main grid is limited by the following constraints:

$$P_{WT\,(PV)}^{min} \leqslant P_{WT\,(PV)}(h) \leqslant P_{WT\,(PV)}^{max} \tag{19}$$

$$P_{grid\_buy}(h) \leqslant u_{grid}(h) \cdot P_{grid\_buy}^{max} \tag{20}$$

$$P_{grid\_sell}(h) \leqslant (1 - u_{grid}(h)) \cdot P_{grid\_sell}^{max} \tag{21}$$

$$P_{grid}(h) = P_{grid\_buy}(h) - P_{grid\_sell}(h) \tag{22}$$

where $P_{WT\,(PV)}^{min\,(max)}$ indicates the minimum (maximum) power that can be obtained from the wind turbine (solar panels). $P_{grid\_buy\,(sell)}^{max}$ indicates the upper limit of power that can be drawn (sold) from (to) the main grid. The point to be taken into consideration here is the criteria for avoiding buying and selling power simultaneously. The binary variable u_{grid} is used to fulfill this requirement. If $u_{grid} = 1$, the power is drawn from the grid and vice versa.

The energy storage unit, which is the most important component of residential MGs, can provide reliable energy during a power outage or store excess energy generated by renewable sources. Batteries are operated according to certain constraints. The first of those is the battery *SoC* level calculated as follows:

$$SoC(h+1) = SoC(h) + (P_{bat}(h) \cdot \Delta h / E_{bat}) \tag{23}$$

where Δh is the timestep of the simulation, E_{bat} is the capacity of the battery. To prolong the battery lifetime, the *SoC* must be kept within certain limits as follows:

$$SoC_{min} \leqslant SoC(h) \leqslant SoC_{max} \tag{24}$$

where $SoC_{min(\max)}$ indicates the minimum (maximum) charge percentage of the battery. Similarly, the charging and discharging powers of the battery should be limited by the following equations:

$$P_{bat}^{ch}(h) \leqslant u_{bat}(h) \cdot P_{bat}^{max\_ch} \cdot \eta_{ch} \tag{25}$$

$$P_{bat}^{dch}(h) \cdot \eta_{dch} \leqslant (1 - u_{bat}(h)) \cdot P_{bat}^{max\_dch} \tag{26}$$

$$P_{bat}(h) = P_{bat}^{ch}(h) - P_{bat}^{dch}(h) \tag{27}$$

where $P_{bat}^{ch\,(dch)}$ indicates the active power that the battery draws (injects) during charging (discharging), $P_{bat}^{max\_ch\,(dch)}$ indicates the maximum charging (discharging) power of the battery, and $\eta_{ch(dch)}$ indicates the charge (discharge) efficiency. The point to be taken into consideration here is the criteria for avoiding charging and discharging simultaneously. The binary variable u_{bat} is used to satisfy this requirement. If it is 1, the battery is charging and vice versa.

The last constraint ensures that the *SoC* value of the battery at the end of each day is equal to its initial value. Thus, a more sustainable EMS can be achieved.

$$SoC(H) = SoC_{initial} \tag{28}$$

4. Case study

4.1. Operation of the residential MG

The analyzed residential MG, which is shown in Fig. 1, consists of two busbars, AC and DC. Since the WT and PV are renewable-based generation units, power converters are designed to extract the maximum power. With the help of maximum power point tracking algorithms such as Perturb&Observe, the maximum power point is determined and appropriate control signals are sent to converters. Therefore, renewable power generation can be estimated by using the solar irradiation, temperature, and wind speed data of the region. The battery is used to ensure the power quality of the DC bus. The voltage level of the DC bus tends to fluctuate due to the connection of RESs and their power variations. To handle this problem, the battery is controlled to keep the voltage of the DC bus constant at *700 V*. It has been shown in previous studies that this level is a good compromise in terms of efficiency, safety, and compatibility with the AC grid [46]. In addition, the surplus energy can be stored in the battery and the power exchange with the main grid can be economically realized. The electric vehicle charging station and lift/lighting units, which are the consumption units, can be considered as DC loads. The last unit is the interlink converter which is controlled by the EMS since it regulates the power exchange with the main grid. The values of parameters for the MG and EMS are given in Table 1.

4.2. Operation of EMS

As explained in Section III, the modules within the EMS produce the outputs required for the optimal operation of the MG by using various inputs. These inputs and outputs are shown in Fig. 8.

The *NILM* module uses the smart meter signals of the participating apartments as the input and extracts the appliance-level data. These data are sent to the *Optimization* module through the *Data Preprocessing* module and then used for Level-1 optimization. Thus, the electricity bill is reduced by considering consumer comfort.

The *Forecast* module estimates renewable energy generation, electric vehicle and lift/lighting power consumption, and consumption of non-participating apartments. These forecasts are sent to the *Optimization* module through the *Data Preprocessing* module and used for Level-2 optimization. Consumption estimates have been obtained using probabilistic models. Renewable generation forecasts were made using historical weather data measured by a weather station, located in the AAU Energy Department at Aalborg University. Undoubtedly, there will be differences between estimates and actual values. This difference has been taken into account during real-time implementation. The actual

Table 1
parameters of the mg and ems [38]

Parameters	Value	Unit	Parameters	Value	Unit
P_{WT}	5	kWp	E_{bat}	80	kWh
P_{PV}	8	kWp	$SoC_{max\,(min)}$	90 (30)	%
P_{EV}	2	kW	$SoC_{initial}$	50	%
V_{dc_bus}	700	V	$P_{bat}^{max\_ch\,(dch)}$	10 (10)	kW
Δt	1	hour	$\eta_{ch\,(dch)}$	87 (90)	%
t_{opt}	15	min	H	6, 12, 24	hour
w_1	0.60		w_2	0.40	
Number of Apartments	16				

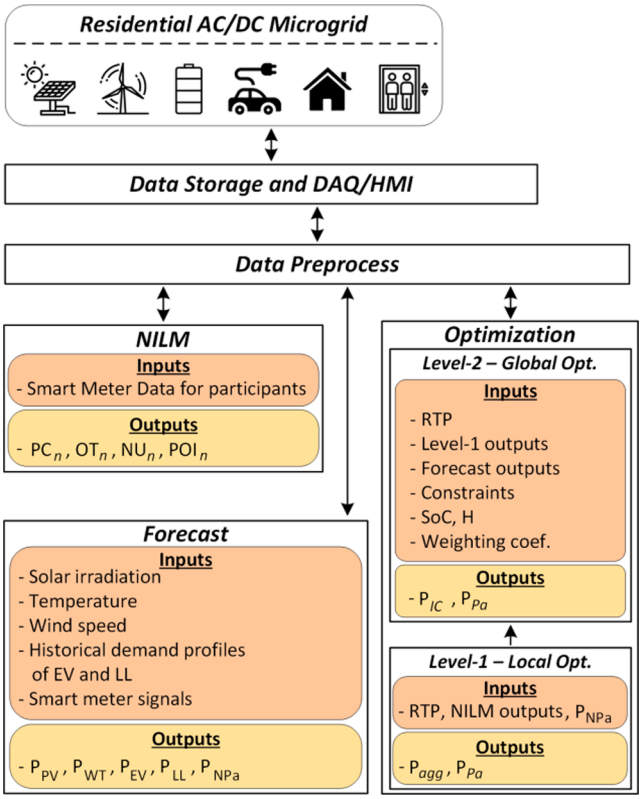

Fig. 8. Data flow between EMS modules.

generation and consumption profiles have been emulated and sent to the test-bed by adding random errors within ±30% of the forecasted value.

Fig. 9 represents the Pareto front of the Level-2 optimization problem and the best compromise solution from the point of view of a conservative decision-maker as discussed in Section III-D-2. The minimum and maximum values of F_1 and F_2 used for linear fuzzy membership function calculation are empirically determined as 1100–1500 and 0–10, respectively. The weighting coefficients related to the best compromise solution ($w_1 = 0.60$, $w_2 = 0.40$) are then used in the experimental test to validate the performance of the proposed EMS framework.

To observe the effect of different optimization horizons (H) on the proposed EMS performance, horizons of 6, 12, and 24 h with a time slot

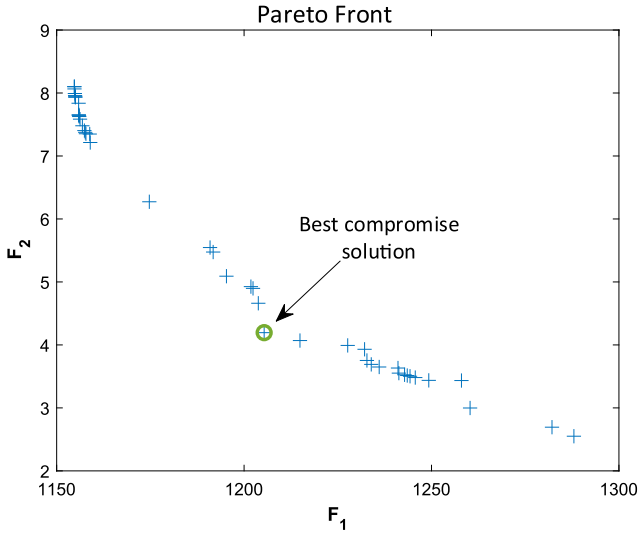

Fig. 9. Pareto front for the Level-2 optimization.

$\Delta h = 1$ h were chosen for optimization. As shown in Fig. 4, the optimization process is performed every $t_{opt} = 15$ min and new set-points are sent to the MG. Therefore, optimization inputs need to be updated accordingly. It was assumed that the RTP information is shared with consumers the day before by the utility grid operator.

5. Experimental results

5.1. System description

The residential MG and the proposed EMS have been tested in real-time at Aalborg University, AAU Energy, AC/DC Microgrid Laboratory. The experimental setup, which is shown in Fig. 10, has been used to test the proposed EMS. The real-time platform consists of a 3-phase isolation transformer (12.5kVA, 400 V) for grid connection, four 2.2 kW 3-phase AC/DC power converters for power conversion, four LCL filters (8.6mH, 4.5μF, 1.8mH), and a dSPACE DS1006 processor board. Since the analyzed MG is grid-connected, it has been assumed that the voltage and frequency values of the AC busbar are regulated by the main grid. Due to the hardware limitations, the DC part of the MG is emulated in the laboratory environment using four AC/DC inverters, which are connected to the same DC bus. While one of the inverters emulates renewable energy generation ($P_{PV} + P_{WT}$), another represents the consumption of the electric vehicle and lift/lighting ($P_{EV} + P_{LL}$). These inverters operate in grid-feeding mode. By following the active and reactive power reference values, they can inject/absorb current into/from the grid. The third inverter is responsible for emulating the battery to regulate the DC bus voltage. For this reason, it's designed as a grid-forming inverter. The last inverter is used as an interlink inverter to emulate the power exchange between the AC and DC buses. In case the SoC is below the lower limit, the grid regulates the DC bus voltage through the interlink inverter. The inverters are controlled using nested control loops, where the inner current loop controls the output current of the inverter and the outer control loop is responsible for generating reference current values $I^*_{\alpha,\beta}$ as a function of voltage, active, and reactive power references (V^*, P^*, Q^*). To generate a reference current value synchronized with the main grid, Clarke transformation is applied by using the phase angle of the grid voltage obtained from the phase-locked loop, and the reference current values are obtained within the $\alpha\beta$ static reference frame [47].

All local controllers for inverters are designed with Matlab/Simulink on a control station. Moreover, the EMS is coded and implemented in a

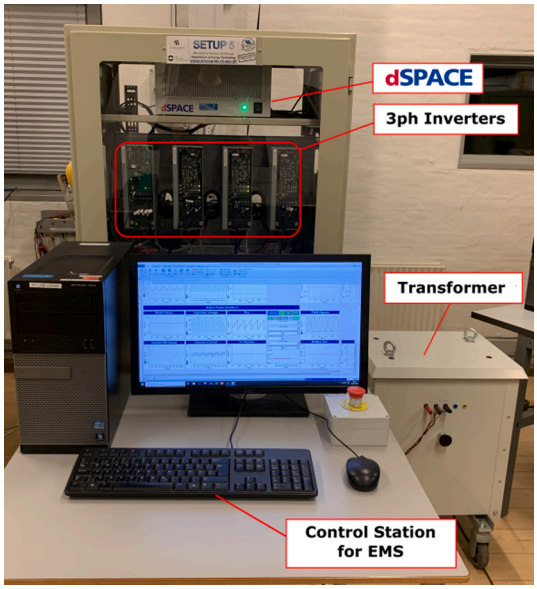

Fig. 10. Experimental setup.

Matlab script. For the optimization process, the general algebraic modeling language (GAMS) is used. The EMS sends the required data to GAMS every 15 min, requesting optimization to be performed. The outputs of GAMS are read by Matlab and sent to the test-bed. The communication between the control station and the real-time platform is provided through a User Datagram Protocol over ethernet. Due to the hardware limitations, all the power values (generation, consumption, etc.) used in the EMS process were scaled down by a factor of 30. In addition, the time was scaled down such that 1 h:2 min for applicability.

5.2. NILM outputs

In this module, the smart meter signals of the apartments are analyzed and the consumption habits of the users are extracted. The energy consumption of the 16 apartments in the residential MG is modeled using the consumption data in the REFIT dataset [48]. The REFIT dataset includes the total consumption and appliance-level consumption data of twenty different households measured in watts at 8-second intervals. For the simplicity of the study, three of the houses which are specified as House 2, 3, and 15 in the data set were chosen for analysis considering the number of occupants, the shiftable appliances in the house, and the recording quality of the data. The consumption profiles of the 16 houses in the residential MG were generated by randomly shifting the consumption profiles of these three houses forward or backward on the time axis. For the analysis, only high power devices such as washing machines (WM), dishwashers (DW), and dryers (DR) were considered. House 3 and 15 have all three appliances, while House 2 has only WM and DW. A deep learning model was trained for each appliance. It is assumed that half of the apartments participate in appliance scheduling and the smart meter signals of these consumers were analyzed. Following this analysis, the energy consumption habits of the users were obtained. After the analysis for House 2, the *POI* parameter which shows the most frequently used periods of the device was obtained by using a probability density function as shown in Fig. 11.

The blue line in Fig. 11 is obtained using actual data, showing which time of day the appliance is preferred to be used. The yellow line shows the result obtained from the NILM analysis. As seen in Fig. 11, the probability of daily use was obtained with high accuracy. The peaks in the curve indicate the periods in which the device is used most frequently. However, many different peaks can be found in the figure. In this paper, peaks that are less than 50% of the maximum peak are not considered. The dashed red lines describe the period interval in which the device is used most frequently. The same graph for House 3 and 15 is shown in Fig. 12.

Other parameters required to schedule the appliances were obtained

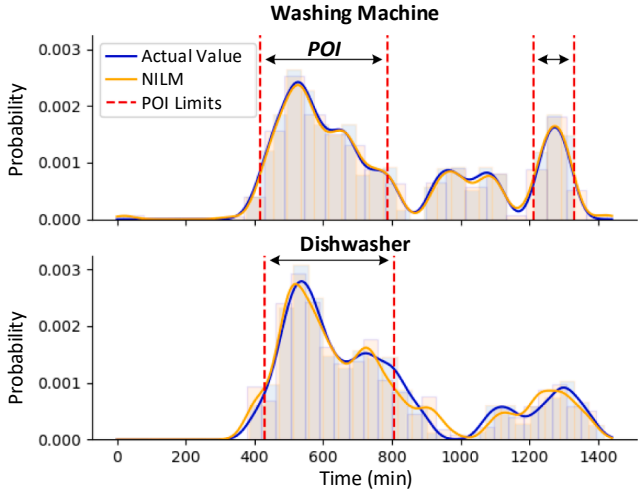

Fig. 11. Preferred operational intervals of House-2.

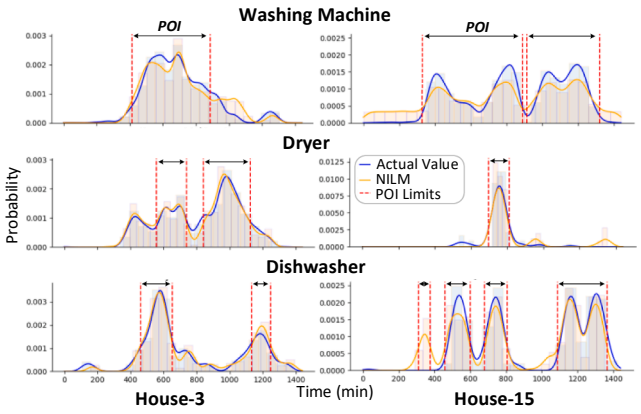

Fig. 12. Preferred operational intervals of House-3 and 15.

as shown in Table 2.

When Table 2 is examined, it is observed that the *OT*, *NU,* and *PC* were estimated with 96%, 78%, and 94% accuracy, respectively. All these results show that NILM analysis can be useful to obtain the appliance-level parameters. By using this data, it is possible to create a more advanced and autonomous EMS. When the *NU* values are examined, it is seen that House-15 rarely uses home appliances (Dryer-almost once in 5 days). This is because there is only one occupant in House-15 while there are more occupants in other houses. To use *NU* within EMS, the real-time application should be done at least for one week. However, in this paper, real-time implementation was carried out only for 24 h. For this reason, the *NU* value is determined as 1 for all devices.

5.3. EMS outputs

As explained in Section D, the consumption profiles of the participating apartments are scheduled by performing local optimization. The consumption profiles of non-participant users are determined with the help of the *Forecast* module. Since the main purpose is to determine the consumption profile of the next day, this process is applied only once each day. The total consumption data of 16 flats are shown in Fig. 13 (a), while the RTP used in the optimization is shown in (b). For the RTP graph, *T1* indicates the periods when the price of electricity is low and *T2* is the high-price interval. Renewable energy generation forecasts and actual values are shown in Fig. 14.

For the real-time test, generation and consumption values are modeled by converters at intervals of 5 min (10 s with scaling). The forecasted load and generation profiles of the MG represented in Fig. 13 and Fig. 14 are used for optimization, while the actual data are used for real-time implementation. Therefore, the differences that may occur between the forecast and real-time measurements are also taken into account. These differences are compensated by the battery. Another important parameter for EMS is the optimization horizon *H*. In this paper, 3 different horizons, 6, 12, and 24 h, have been considered to observe the effect of *H* on the results.

Table 2
Appliance parameters of Houses 2, 3, and 15

Houses	App.	OT (min)		NU		PC (W)	
		Actual	NILM	Actual	NILM	Actual	NILM
House 2	WM	107	108	0.5	0.5	275	261
	DW	115	114	0.7	0.65	704	680
House 3	WM	81	70	0.875	0.685	435	385
	DW	73	72	0.8	0.725	1083	1041
	DR	80	79	0.35	0.25	1387	1538
House 15	WM	99	105	0.4	0.35	552	606
	DW	95	92	0.2	0.1	554	582
	DR	90	93	0.2	0.1	1475	1537

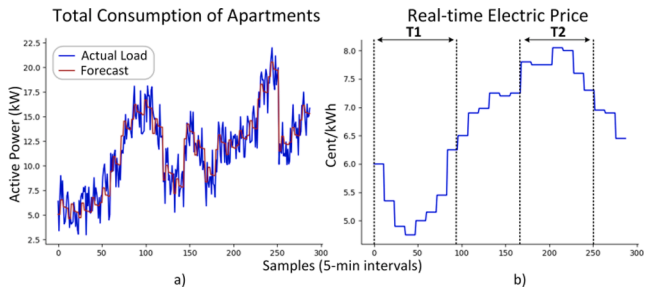

Fig. 13. Total power consumptions of apartments and RTP.

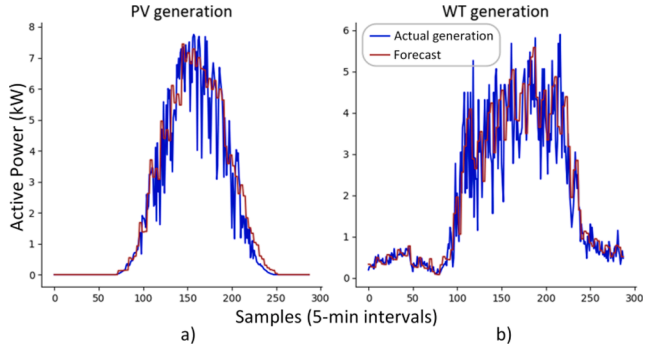

Fig. 14. Renewable energy generation.

In addition, a peak shaving strategy is implemented as a benchmark. This strategy ensures that the power drawn from the grid remains below a threshold level. As long as the absorbed power is below the threshold, there will be no power exchange between the AC and DC buses. When the threshold is exceeded, the required amount of energy is transferred from the DC bus to the AC bus. Meanwhile, if the SoC of the battery goes beyond the limit values in (24), the required amount of power will be transferred from the AC bus to the DC bus (in case of $SoC < SoC_{min}$) or vice versa, and constraint (24) is guaranteed. In this paper, the threshold value is set to 16 kW. It is worth mentioning that the Level-1 optimization is also implemented in the peak-shaving strategy.

The obtained results were compared by considering the average time spent for each optimization, operation cost F_1, *std* F_2, and the Level-2 multi-objective function OF_2 values as shown in Table 3.

In Table 3, the second column related to the optimization time shows the average time of solving the optimization problem every 15 min. It is observed that the shorter the horizon, the shorter the average optimization time. Since a 24-hour optimization has a wider search space, the calculation time is longer as expected. The average calculation time of the 24-hour horizon was measured as 0.539 s, which is good enough for a real-time application.

When the F_1 values obtained in the experiments are compared, it is seen that the optimal cost is $1416.49 for the 24-hour horizon. In contrast, the higher cost was achieved with the peak shaving strategy due to the operation without optimization. The proposed EMS provides a 12.36% reduction in operating cost compared to the peak shaving strategy. As can be seen in Table 3, in 24-hour optimization, the total objective value (OF_2) value is less than other horizons. The reason lies in the fact that the operating schedules are made based on a longer view, thereby more information about the future operating conditions are considered. If electricity price of the next 24 h is taken into account while optimizing, the cheapest hours of the day can be determined and the battery can be charged at those hours, and the stored energy can be used during the hours when the RTP is high. However, if only the RTP of the next 6 h is available, the optimization is made by ignoring the cheaper periods. For this reason, the battery may be charged in expensive periods, and the cost and hence the total objective value increases. However, as the horizon gets longer, the accuracy of the forecasts may decrease, which may prevent the optimization to find a global optimum solution. For this reason, the extension of the optimization horizon may not always constitute an advantage and a satisfactory trade-off is required. According to Table 3, the best std value for the received power from the grid belongs to the case with 12-hour optimization horizon. It is worth noticing that there is a difference between the cost of the best compromise solution and the cost values obtained in the experimental tests. The reason is that the Pareto front in Fig. 9 is obtained with offline simulation considering forecasted values for consumer load and renewable power generation and the power loss of converters is neglected. While in the experimental tests, the realized values are taken into account and there is power loss in the system.

Table 3
Experimental results for a residential mg

Opt. Horizon	Opt. time (s)	F_1 (cent)	F_2 (watt)	OF_2
Peak Shaving	–	1616.21	4.068	0.937
6 h	0.377	1496.05	4.112	0.759
12 h	0.380	1492.37	**3.525**	0.729
24 h	0.539	**1416.49**	4.301	**0.647**

Fig. 15 shows the EMS outputs obtained for each experiment. In the first row of Fig. 15, the power exchange with the main grid, in the second row the power exchange of the interlink converter, and in the last row the *SoC* value of the battery are represented. Undoubtedly, the most important factor affecting the operation cost of the MG is RTP. Power exchange with the main grid will be regulated according to RTP and the battery will be operated in an optimum way. Therefore, the charging and discharging state of the battery will significantly affect the operating cost.

In Fig. 15, T1 and T2 represent the periods when the electricity price is cheap and expensive, respectively. In the first column of Fig. 15, the results of the peak shaving strategy, which operates independently from RTP (since no optimization is applied), are depicted. In this strategy, the battery is charged or discharged according to the generation/consumption power values in the DC bus. As seen in Fig. 15, the battery is discharged in the T1 period because there is not enough renewable generation. However, as the generation increases with the sunrise, the battery starts to be charged. Since the SOC exceeds the limit value at the beginning of the T2 period, the surplus energy is transferred to the AC bus via the interlink converter. Meanwhile, when the power drawn from the grid exceeds the threshold of 16 kW, peak shaving is applied by drawing the necessary power from the DC bus. The power exchange between the DC and AC buses can be observed from the second row of Fig. 15.

When the optimization-based EMSs implemented for 6 h, 12 h, and 24 h horizons are examined, different charge/discharge characteristics are observed for the battery depending on the horizon. If the *SoC* variation of the 6-hours horizon is analyzed, it is observed that the SOC value of the battery is stable during the T1 period and increases in the T2 period, which means the battery is charged during the expensive period. The main reason is that RTP information for the whole day is not available for the optimization process. Therefore, the algorithm cannot distinguish between cheap and expensive electricity price periods. Considering the 12-hour optimization, it is observed that the battery is utilized better comparing to the 6-hour case because the RTP for the next 12 h is available. While the battery is partially charged during the T1 period, it desires to increase its SOC value as it gets closer to the T2 period. However, the fact that the SoC value does not reach the upper limit of 90% indicates that the EMS cannot utilize the battery with its best performance.

When 24-hour optimization is evaluated, it is seen that the battery is almost fully charged during the T1 period, which is the best way to reduce the operation cost of the MG. The SOC of the battery remains relatively stable between the T1 and T2 periods and reaches a high SOC

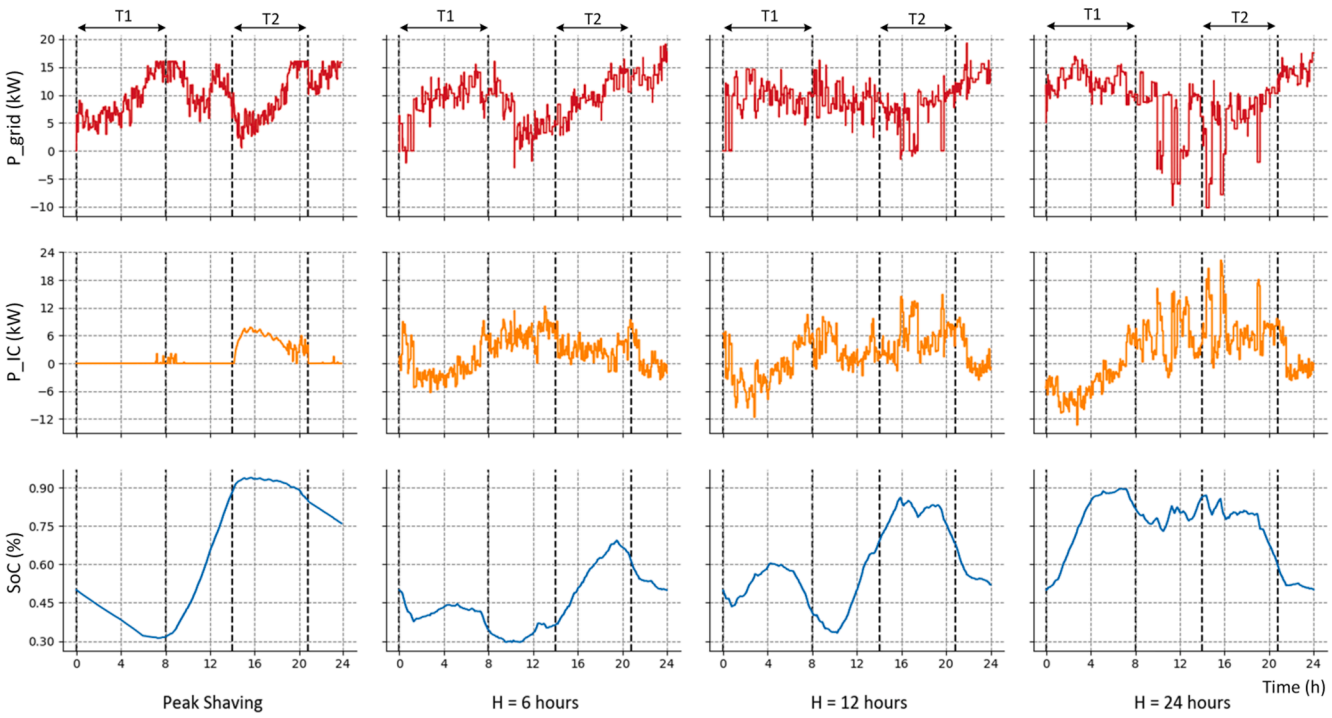

Fig. 15. Experimental results for the residential MG.

value at the beginning of T2 period. Since RTP for the next 24-hour is available, cheap and expensive electricity price periods are distinguished by EMS, and a proper charging strategy is implemented.

In the last hours of the day, the terminal constraint defined by (28) is activated to ensure that the battery starts the next day with the same SoC level as $SoC_{initial}$.

6. Conclusion

Energy management strategies are of great importance for the optimal operation of MGs. In this paper, an advanced system-level EMS designed for a hybrid AC/DC residential MG has been proposed and experimentally validated to efficiently operate a residential MG. Since the analyzed MG has individual households, the smart meter signals of each household have been analyzed with NILM algorithm to extract the consumption profiles of the customers. By using this information, consumers' daily energy costs were minimized at the first level of optimization, by considering their consumption habits. In this way, it was ensured that both consumers' bills were reduced and their comfort levels were not affected. In the second level of optimization, optimum operation of MG was ensured by considering the generation and consumption units of MG. Real-time test results have proven that a 24-hour optimization horizon provides more optimal operation than 6 and 12-hour horizons. Experiments have shown that the battery cannot be fully charged when using a 6-hour horizon, thus increasing the operating cost. In the 24-hour horizon, the battery could be fully charged, thus minimizing the operating cost of the MG. In addition, thanks to the PAR function included in the multi-objective optimization problem, the power drawn from the utility grid is smoothed.

As a limitation of the proposed method, deep learning-based approaches require large amounts of labeled data in case they are trained in a supervised manner. However, obtaining labeled data may not always be practical. To mitigate this problem, new approaches trainable with limited data should be developed. Another limitation of the proposed NILM strategy is the lack of an updating mechanism. Some appliance parameters such as the average number of daily uses (NU) and the most preferred operation interval (POI) should be continuously updated since these parameters may vary depending on the seasonality and other factors. This limitation will be addressed in future work of the authors.

CRediT authorship contribution statement

Halil Cimen: Conceptualization, Methodology, Software, Validation. **Najmeh Bazmohammadi:** Conceptualization, Formal analysis, Software, Validation. **Abderezak Lashab:** Validation, Investigation. **Yacine Terriche:** Writing – review & editing, Visualization. **Juan C. Vasquez:** Supervision, Project administration. **Josep M. Guerrero:** Supervision, Project administration.

Declaration of Competing Interest

The authors declare that they have no known competing financial interests or personal relationships that could have appeared to influence the work reported in this paper.

Acknowledgements

This work was supported by VILLUM FONDEN under the VILLUM Investigator Grant (no. 25920): Center for Research on Microgrids (CROM); www.crom.et.aau.dk and the AAU Talent Project-The Energy Internet-Integrating Internet of Things into the Smart Grid (771116) and The Scientific and Technological Research Council of Turkey BIDEB-2214 International Doctoral Research Fellowship Programme.

The authors thank Emilio José Palacios-García and Enrique Rodriguez-Diaz for helping with the experimental configuration.

References

[1] Elkazaz M, Sumner M, Naghiyev E, Pholboon S, Davies R, Thomas D. A hierarchical two-stage energy management for a home microgrid using model predictive and real-time controllers. Appl Energy 2020;269:115118.

[2] Pascual J, Arcos-Aviles D, Ursúa A, Sanchis P, Marroyo L. Energy management for an electro-thermal renewable–based residential microgrid with energy balance forecasting and demand side management. Appl Energy 2021;295:117062.

[3] Ran X, Leng S. Enhanced robust index model for load scheduling of a home energy local network with a load shifting strategy. IEEE Access 2019;7:19943–53.
[4] Salgado M, Negrete-Pincetic M, Lorca Á, Olivares D. A low-complexity decision model for home energy management systems. Appl Energy 2021;294:116985.
[5] Wang D, Zhang X, Qu K, Yu T, Pan Z, Liu Q. Pareto tribe evolution with equilibrium-based decision for multi-objective optimization of multiple home energy management systems. Energy Build 2018;159:11–23.
[6] Pilloni V, Floris A, Meloni A, Atzori L. Smart home energy management including renewable sources: A qoe-driven approach. IEEE Trans Smart Grid 2016;9(3):2006–18.
[7] Hansen TM, Roche R, Suryanarayanan S, Maciejewski AA, Siegel HJ. Heuristic optimization for an aggregator-based resource allocation in the smart grid. IEEE Trans Smart Grid 2015;6(4):1785–94.
[8] Scheller F, Burkhardt R, Schwarzeit R, McKenna R, Bruckner T. Competition between simultaneous demand-side flexibility options: the case of community electricity storage systems. Appl Energy 2020;269:114969.
[9] Hart GW. Nonintrusive appliance load monitoring. Proc IEEE 1992;80(12):1870–91.
[10] Cimen H, Palacios-Garcia EJ, Kolaek M, Cetinkaya N, Vasquez JC, Guerrero JM. Smart-Building Applications: Deep Learning-Based, Real-Time Load Monitoring. IEEE Ind Electron Mag 2021;15(2):4–15. https://doi.org/10.1109/MIE.2020.3023075.
[11] Himeur Y, Ghanem K, Alsalemi A, Bensaali F, Amira A. Artificial intelligence based anomaly detection of energy consumption in buildings: A review, current trends and new perspectives. Appl Energy 2021;287:116601.
[12] Y. Han, Y. Xu, Y. Huo, and Q. Zhao, "Non-intrusive load monitoring by voltage–current trajectory enabled asymmetric deep supervised hashing," IET Generation, Transmission & Distribution, 2021.
[13] Bonfigli R, Principi E, Fagiani M, Severini M, Squartini S, Piazza F. Non-intrusive load monitoring by using active and reactive power in additive Factorial Hidden Markov Models. Appl Energy 2017;208:1590–607.
[14] Kim H, Marwah M, Arlitt M, Lyon G, Han J. In: SIAM; 2011. p. 747–58.
[15] Kolter JZ, Jaakkola T. Approximate inference in additive factorial hmms with application to energy disaggregation. In: in Artificial Intelligence and Statistics; 2012. p. 1472–82.
[16] Kong W, Dong ZY, Hill DJ, Ma J, Zhao J, Luo F. A hierarchical hidden markov model framework for home appliance modeling. IEEE Trans Smart Grid 2016;9(4):3079–90.
[17] Parson O, Ghosh S, Weal M, Rogers A. An unsupervised training method for non-intrusive appliance load monitoring. Artif Intell 2014;217:1–19.
[18] Zoha A, Gluhak A, Imran M, Rajasegarar S. Non-intrusive load monitoring approaches for disaggregated energy sensing: A survey. Sensors 2012;12(12):16838–66.
[19] Himeur Y, Alsalemi A, Bensaali F, Amira A. Robust event-based non-intrusive appliance recognition using multi-scale wavelet packet tree and ensemble bagging tree. Appl Energy 2020;267:114877.
[20] Liu Y, Liu W, Shen Y, Zhao X, Gao S. Toward smart energy user: Real time non-intrusive load monitoring with simultaneous switching operations. Appl Energy 2021;287:116616.
[21] Himeur Y, Alsalemi A, Bensaali F, Amira A. Smart non-intrusive appliance identification using a novel local power histogramming descriptor with an improved k-nearest neighbors classifier. Sustainable Cities and Society 2021;67:102764.
[22] Ahmed AM, Zhang Y, Eliassen F. In: IEEE; 2020. p. 1–7.
[23] A. Harell, R. Jones, S. Makonin, and I. V. Bajic, "PowerGAN: Synthesizing Appliance Power Signatures Using Generative Adversarial Networks," arXiv preprint arXiv:2007.13645, 2020.
[24] Xia M, Liu W, Wang Ke, Zhang Xu, Xu Y. Non-intrusive load disaggregation based on deep dilated residual network. Electr Power Syst Res 2019;170:277–85.
[25] Zhao B, Ye M, Stankovic L, Stankovic V. Non-intrusive load disaggregation solutions for very low-rate smart meter data. Appl Energy 2020;268:114949.
[26] Hochreiter S, Schmidhuber J. Long short-term memory. Neural Comput 1997;9(8):1735–80.
[27] Goodfellow I, Bengio Y, Courville A. Deep learning. MIT press 2016.
[28] Rafiq H, Shi X, Zhang H, Li H, Ochani MK, Shah AA. Generalizability Improvement of Deep Learning-Based Non-Intrusive Load Monitoring System Using Data Augmentation. IEEE Trans Smart Grid 2021;12(4):3265–77.
[29] Z. Zhou, Y. Xiang, H. Xu, Y. Wang, and D. Shi, "Unsupervised Learning for Non-Intrusive Load Monitoring in Smart Grid Based on Spiking Deep Neural Network," Journal of Modern Power Systems and Clean Energy, 2021.
[30] Chelli G, Ciabattoni L, Flores-Arias J, Foresi G, Monteriù A, Pagnotta DP. In: IEEE; 2018. p. 1–2.
[31] Lin Y-H, Tsai M-S. An advanced home energy management system facilitated by nonintrusive load monitoring with automated multiobjective power scheduling. IEEE Trans Smart Grid 2015;6(4):1839–51.
[32] Cimen H, Cetinkaya N, Vasquez JC, Guerrero JM. A Microgrid Energy Management System based on Non-Intrusive Load Monitoring via Multitask Learning. IEEE Trans Smart Grid 2021;12(2):977–87.
[33] H. Yue, K. Yan, J. Zhao, Y. Ren, X. Yan, and H. Zhao, "Estimating Demand Response Flexibility of Smart Home Appliances via NILM Algorithm," in 2020 IEEE 4th Information Technology, Networking, Electronic and Automation Control Conference (ITNEC), 2020, vol. 1: IEEE, pp. 394-398.
[34] Azizi E, et al. Residential Energy Flexibility Characterization Using Non-intrusive Load Monitoring. Sustainable Cities and Society 2021:103321.
[35] Rehman AU, Lie TT, Vallès B, Tito SR. Non-invasive load-shed authentication model for demand response applications assisted by event-based non-intrusive load monitoring. Energy and AI 2021;3:100055.
[36] Guerrero JM, Vasquez JC, Matas J, de Vicuna LG, Castilla M. Hierarchical control of droop-controlled AC and DC microgrids—A general approach toward standardization. IEEE Trans Ind Electron 2011;58(1):158–72.
[37] Agency IE. Electricity Information: Overview 2020.
[38] Rodriguez-Diaz E, Palacios-Garcia EJ, Anvari-Moghaddam A, Vasquez JC, Guerrero JM. In: IEEE; 2017. p. 256–61.
[39] Fairley P. DC versus AC: The second war of currents has already begun [in my view]. IEEE Power Energ Mag 2012;10(6):104–1103.
[40] Zia MF, Elbouchikhi E, Benbouzid M. Microgrids energy management systems: A critical review on methods, solutions, and prospects. Appl Energy 2018;222:1033–55.
[41] Aydin E, Brounen D, Kok N. Information provision and energy consumption: Evidence from a field experiment. Energy Econ 2018;71:403–10.
[42] Çimen H, Çetinkaya N. Voltage sensitivity-based demand-side management to reduce voltage unbalance in islanded microgrids. IET Renew Power Gener 2019;13(13):2367–75.
[43] Anvari-Moghaddam A, Guerrero JM, Vasquez JC, Monsef H, Rahimi-Kian A. Efficient energy management for a grid-tied residential microgrid. IET Gener Transm Distrib 2017;11(11):2752–61.
[44] Zaro F, Abido MA. In: IEEE; 2011. p. 1122–7.
[45] Soroudi A, Afrasiab M. Binary PSO-based dynamic multi-objective model for distributed generation planning under uncertainty. IET Renew Power Gener 2012;6(2):67–78.
[46] Rodriguez-Diaz E, Chen F, Vasquez JC, Guerrero JM, Burgos R, Boroyevich D. Voltage-level selection of future two-level LVdc distribution grids: A compromise between grid compatibiliy, safety, and efficiency. IEEE Electrif Mag 2016;4(2):20–8.
[47] Golestan S, Ramezani M, Guerrero JM, Freijedo FD, Monfared M. Moving Average Filter Based Phase-Locked Loops: Performance Analysis and Design Guidelines. IEEE Trans Power Electron 2014;29(6):2750–63. https://doi.org/10.1109/TPEL.2013.2273461.
[48] Murray D, Stankovic L, Stankovic V. An electrical load measurements dataset of United Kingdom households from a two-year longitudinal study. Sci Data 2017;4:160122.